Journal of Power Sources 217 (2012) 485–490

Contents lists available at SciVerse ScienceDirect

Journal of Power Sources

journal homepage: www.elsevier.com/locate/jpowsour

FeAl-based coatings deposited by high-energy micro-arc alloying process for wet-seal areas of molten carbonate fuel cell

P.Y. Guo [a,b], C.L. Zeng [a,*], N. Wang [b], Y. Shao [b]

[a] State Key Laboratory for Corrosion and Protection, Institute of Metal Research, Chinese Academy of Science, Shenyang 110016, China
[b] Jiangsu Provincial Key Laboratory of Advanced Welding Technology, Jiangsu University of Science and Technology, Jiangsu 212003, China

HIGHLIGHTS

- FeAl coatings for wet-seal materials of molten carbonate fuel cell were studied.
- High-energy micro-arc alloying process was employed to prepare FeAl coatings.
- FeAl coatings are microcrystalline, with a metallurgic bonding to the substrate.
- FeAl coatings have significantly larger impedance values than 316 stainless steel.
- FeAl coatings increase greatly the corrosion resistance of 316 stainless steel.

ARTICLE INFO

Article history:
Received 3 April 2012
Received in revised form
12 June 2012
Accepted 13 June 2012
Available online 20 June 2012

Keywords:
Molten carbonate fuel cell
Wet-seal area
High-energy micro-arc alloying process
Iron aluminide coating
Corrosion
Electrochemical impedance spectroscopy

ABSTRACT

The corrosion of bipolar plates is a great obstacle to the industrial application of molten carbonate fuel cell (MCFC). No electrical conductivity is needed for the wet-seal materials, thus the application of aluminum coatings is a very effective method to inhibit the corrosion of wet-seal areas of MCFC by the formation of a protective Al_2O_3 scale. In this work, a high-energy micro-arc alloying (HEMAA) process is attempted to prepare FeAl coatings on the type 316 stainless steel (316SS) as wet-seal material of MCFC using an FeAl intermetallic compound rod as the deposition electrode. The microstructure of the FeAl coatings is analyzed, and its corrosion behavior in molten $(0.62Li, 0.38K)_2CO_3$ at 650 °C in air is examined by electrochemical impedance spectroscopy. The experimental results indicate that the FeAl coating on 316SS is microcrystalline, with a metallurgic bonding with the substrate. The Nyquist plots for the corrosion of both the bare and the coated steel are all composed of double capacitive loops, but with significantly larger impedance values observed for the coated steel. The FeAl coatings increase greatly the corrosion resistance of 316SS by forming a compact and adhesive Al_2O_3 scale.

1. Introduction

Molten carbonate fuel cell (MCFC) is a very attractive power-generation device that converts electrochemically chemical energy of hydrogen (suitable fuels include coal gas, liquefied petroleum gas, methanol, and even natural gas) and oxygen into electricity, with the advantages of high efficiency and low emission. USA, Germany, Italy, Japan, Korea, etc. have developed MCFC systems with the power size of several kW to multi-MW. Although great progresses have been made, MCFC still can not reach the commercial goal of at least a 40,000 h lifetime. The corrosion of fuel cell materials [1–3], mainly including the dissolution of the NiO cathode and the corrosion of bipolar plates, is a great obstacle to the industrial use of MCFC.

As a multi-functional component, bipolar plates perform as current conductors between cells, distribute and separate the cathodic and anodic reactant gases. This component is in contact with three quite different corrosion environments, i.e. the cathode area with an oxidizing gas environment, the anode area with a reducing gas environment and the so-called 'wet-seal' region. No single material or coating can meet so different environments [4–6]. The wet-seal materials undergo the most severe corrosion due to the presence of an insidious micro-galvanic corrosion [7]. Austenitic stainless steels are the leading candidates for the bipolar plate materials of MCFC, due to their good mechanic properties, reasonable corrosion resistance, ease of fabrication, low cost, etc. However, these materials still suffer from fast corrosion in the wet-seal environments, and cannot meet the requirements of at least a 40,000 h

* Corresponding author. Tel.: +86 24 23904553; fax: +86 24 23893624.
E-mail address: clzeng@imr.ac.cn (C.L. Zeng).

0378-7753/$ – see front matter © 2012 Elsevier B.V. All rights reserved.
http://dx.doi.org/10.1016/j.jpowsour.2012.06.054

lifetime [8,9]. Fortunately, no electrical conductivity is needed for the wet-seal materials. Therefore, Al_2O_3-forming alloys or coatings can be used in the wet-seal environments. Nevertheless, the direct use of Al-containing alloys as the wet-seal materials is limited by the concentration of aluminum, because the high Al content in alloys needed to form a protective Al_2O_3 scale (which can react with molten Li_2CO_3 to form $LiAlO_2$) would cause poor mechanical properties. Thus, the application of aluminum coatings seems to be a very simple and effective approach to limit corrosion in the wet-seal area due to the formation of a protective $LiAlO_2$ scale.

To protect wet-seals from corrosion, some efforts have been conducted to develop an Al-coating manufacturing process, mainly including thermal spraying [10], slurry [11], and ion vapor deposition (IVD) [12]. Moon etc. [13] also prepared a surface layer of the intermetallic compound Ni_2Al_3 or NiAl on a 316L stainless steel plate by electroplating double layers of nickel and aluminium, followed by heat treatment at 650 or 800 °C for 1 h. The Al-coatings prepared by these methods can reduce significantly the corrosion in the wet-seal area. However, most of these aluminization methods require post-deposition diffusion treatments. Therefore, it is of great significance to develop an easy and low-cost coating process. Recently, a new aluminization method based on the electrospark deposition (ESD) has been proposed to obtain directly a layer of FeAl intermetallic alloy on the type 316L stainless steel [14]. The prominent advantages of this method over IVD and other popular coating technologies such as chemical vapor deposition, slurry and thermal spraying are the possibility of realizing a diffusion coating with a high resistance to spallation and with a minimal thermal distortion [15,16]. Similarly, one of the present authors also introduced a simple and cost-effective high-energy micro-arc alloying (HEMAA) technique to the preparation of pinhole-free coatings for metallic bipolar plates of proton exchange membrane fuel cell, with a metallurgical bonding between the coating and the substrate alloy [17]. In this study, HEMAA was attempted to deposit FeAl coatings on316 stainless steel to be used as wet-seal material of MCFC, and the corrosion behavior of the coated steels was examined by electrochemical impedance technique.

2. Experimental procedures

In the present study, type 316 stainless steel (316 SS) was used as substrate alloy. The steel plates were cut into specimens with the size of 10 × 10 × 1 mm, followed by grinding with 800-grit SiC paper and degreasing with acetone. A rod of the FeAl intermetallic compound (Fe–38.26Al, in atom percent) with a diameter of 4 mm was used as the deposition electrode. To avoid heating and oxidation during deposition, the substrate area was kept at room temperature by a strong jet of argon gas. With a succession of pulse discharge depositing operation under the conditions of low voltage (60 ~ 80 V) and high frequency (1000 ~ 2000 Hz), a FeAl alloy layer was obtained on 316 SS.

A two-electrode system (two working electrodes) was employed for electrochemical impedance measurements. The preparation of the working electrode is as follows. A Fe–Cr wire was spot-welded to one end of the specimen for electric connection. The welding ends of two specimens spaced were sealed in an alumina tube with high temperature cement, as shown in Fig. 1. After the cement was dried at room temperature, it was further solidified at 100 °C for 24 h and then at 350 °C for 10 h, respectively. Then, the electrode surface was polished again by 800 grit SiC paper, degreased and dried.

Electrochemical impedance measurements at open circuit were carried out at 650 °C in an eutectic $(0.62Li, 0.38K)_2CO_3$ (mole fraction) melt in air between 0.01 Hz and 100 kHz with PAR 2273 Potentiostat/Galvanostat. The amplitude of input sin-wave voltage was 10 mV. After drying 80 g of the $(Li,K)_2CO_3$ mixture contained in an alumina crucible at 350 °C for 24 h, the furnace was heated to 650 °C.

Scanning electron microscopy (SEM) coupled with energy dispersive X-ray microanalysis (EDX), and X-ray Diffraction (XRD) were used to characterize the coatings and the corrosion products.

3. Results and discussion

3.1. Characterizations of coatings

Fig. 2 shows the microstructures of the cast FeAl intermetallic compound used as the deposition electrode and the as-prepared FeAl coating on 316SS, respectively. HEMAA produced a microcrystalline coating with a grain size much smaller than that for the cast FeAl intermetallic compound. Fig. 3 shows the cross-sectional morphology of the as-prepared FeAl coating on 316SS. It is shown clearly that a continuous Al-containing coating has been produced on the alloy surface, with a metallurgical bonding between the coating and the substrate alloy. Except for some micro pores, oxides

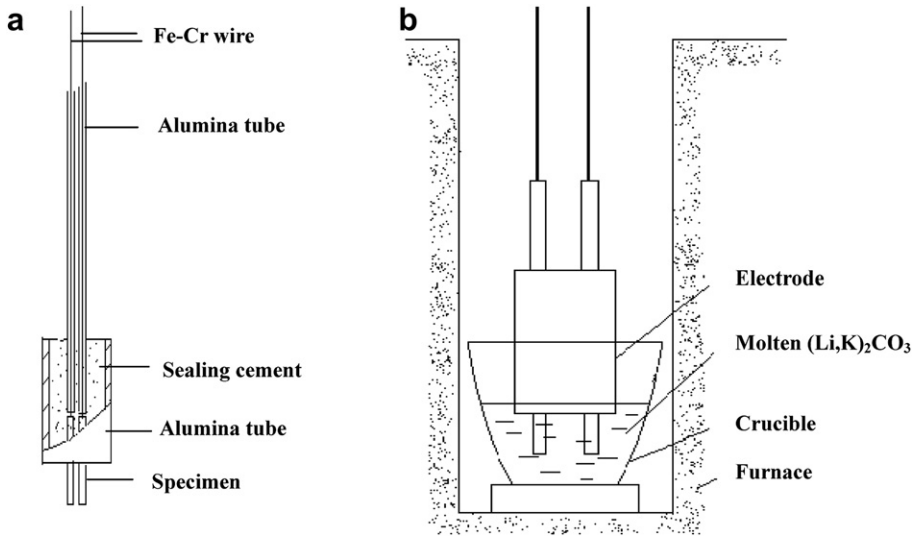

Fig. 1. Two-electrode arrangement for electrochemical impedance measurements.

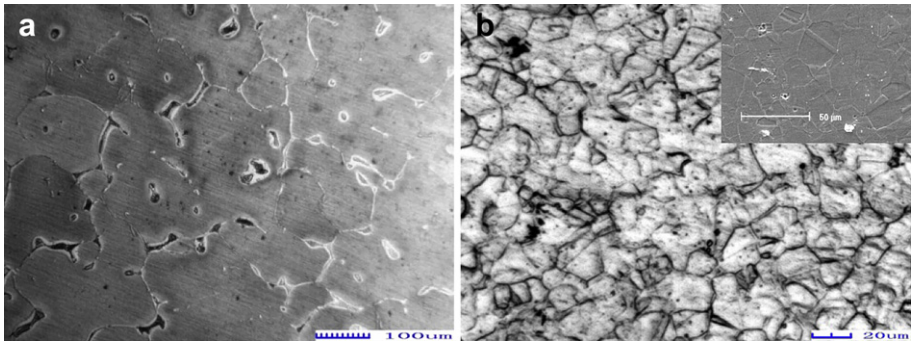

Fig. 2. Microstructures of the cast FeAl electrode (a) and the as-prepared FeAl coating on 316SS (b).

and penetrating cracks were not observed in the coating. EDX analysis revealed that the Al content of the coating tended to decrease with the distance from the surface of the coating. Additionally, small amounts of Ni and Cr were also detected, due to the occurrence of mass transfer between the coating and the substrate during HEMAA, by which Fe and Al transfer from the FeAl electrode to the substrate, and some elements such as Fe, Ni and Cr from the substrate to the coating layer.

3.2. Electrochemical impedance spectra

Fig. 4 shows the typical Nyquist and Bode plots for the corrosion of 316SS in molten $(Li,K)_2CO_3$ at 650 °C after various exposure times. The Nyquist plots were composed of double capacitive loops, i.e. a very small semi-circle at high frequencies and a large semi-circle at low-frequency port during the experimental duration of 24 h. It is noted that the time constant in the high-frequency port could not be characterized clearly, especially in the initial stage. The impedance value for 316SS changed little with exposure time. Fig. 5 gives the typical Nyquist and Bode plots for the corrosion of the FeAl-coated 316SS in molten $(Li,K)_2CO_3$ after various exposure times. The Nyquist plots also consisted of double capacitive loops, just as observed for the bare 316SS, but with significantly larger impedance values, suggesting the effectiveness of FeAl coating in inhabiting the corrosion of 316SS. Additionally, differing from the bare steel, two time constants are shown clearly in the Bode plots for the coated steel.

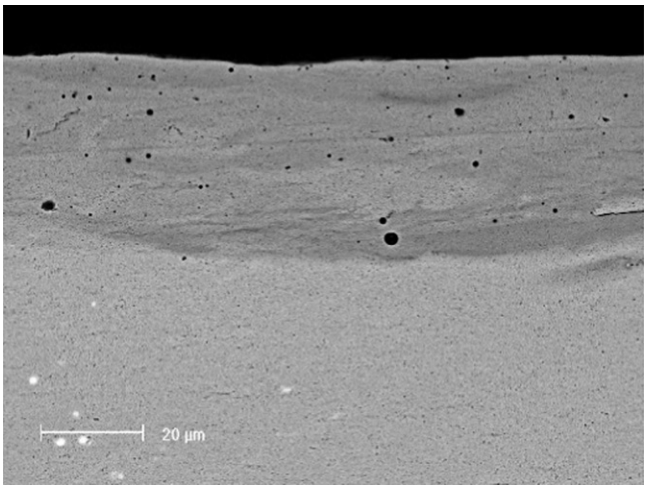

Fig. 3. Cross-sectional morphology of the as-prepared FeAl coating on 316SS.

3.3. Corrosion products

Fig. 6 shows the X-ray diffraction patterns for the corrosion products formed on the bare and FeAl-coated 316 SS, respectively. The corrosion products formed on the FeAl coating are composed of Fe_2O_3 and Al_2O_3, while those grown on 316SS mainly consist of Fe_2O_3 and Cr-rich oxides (Cr_2O_3, $FeCr_2O_4$).

Fig. 7(a,b) gives the cross-sectional morphologies of 316SS corroded in molten $(Li,K)_2CO_3$ at 650 °C for 24 h. The scale exhibits a bi-layered microstructure composed of external bright Fe_2O_3 and inner gray Cr-rich oxides ($FeCr_2O_4$, Cr_2O_3). Moreover, a Cr-depleted zone was formed beneath the scale. Fig. 7c shows the cross-sectional morphology of the FeAl-coated 316SS after corrosion in the melt at 650 °C for 24. Clearly, a thin (less than 3 μm) bi-layered scale composed of external Fe_2O_3 (bright) and inner Al_2O_3(dark) has formed on the coated steel. Beneath the scale an Al-depleted zone was also produced. The significantly increased corrosion resistance of FeAl coating prepared by HEMAA is ascribed to the formation of a continuous and adhesive Al_2O_3 scale.

3.4. Interpretation of EIS spectra

The Nyquist plots for the corrosion of the bare and coated 316 SS are all composed of two depressed semicircles, and a continuous Al_2O_3 scale has formed on the coated steel and a Cr-rich scale on the bare steel. This Al-rich or Cr-rich scale is effective in inhibiting the corrosion.

The corrosion of the bare and FeAl-coated 316SS in molten $(Li,K)_2CO_3$ at 650 °C in air includes oxidation and reduction processes. The reduction of oxygen is the main reduction reaction. It has been accepted that oxygen takes part in reduction reaction in the form of chemically dissolved oxygen, not physically dissolved oxygen [18,19]. The chemically dissolved oxygen diffuses to the alloy/melt interface to be reduced to O^{2-}. For corrosion in molten salts, the transportation of ions in the scale and the diffusion of oxidants in the melt may become rate-limiting process, which will further depend on the protection of the scale formed on the alloy surface. Our previous study indicated that when a non-protective scale was formed on the alloy surface in molten $(Li,K)_2CO_3$, a Warburg impedance was observed at low frequencies, and the corrosion of alloys was controlled by the diffusion of oxidants in the melt [20]. When a protective scale was formed on the alloy surface, however, the Nyquist plots were composed of double capacitive loops, and the corrosion of alloys was controlled by the diffusion of ions through the scale. In the present study, the corrosion of the bare and coated steel is controlled by the diffusion of species through the scale due to the formation of a protective Cr-rich or Al-rich scale. Thus a serial equivalent circuit was proposed to fit the impedance spectra, as shown in Fig. 8, where R_s represents the

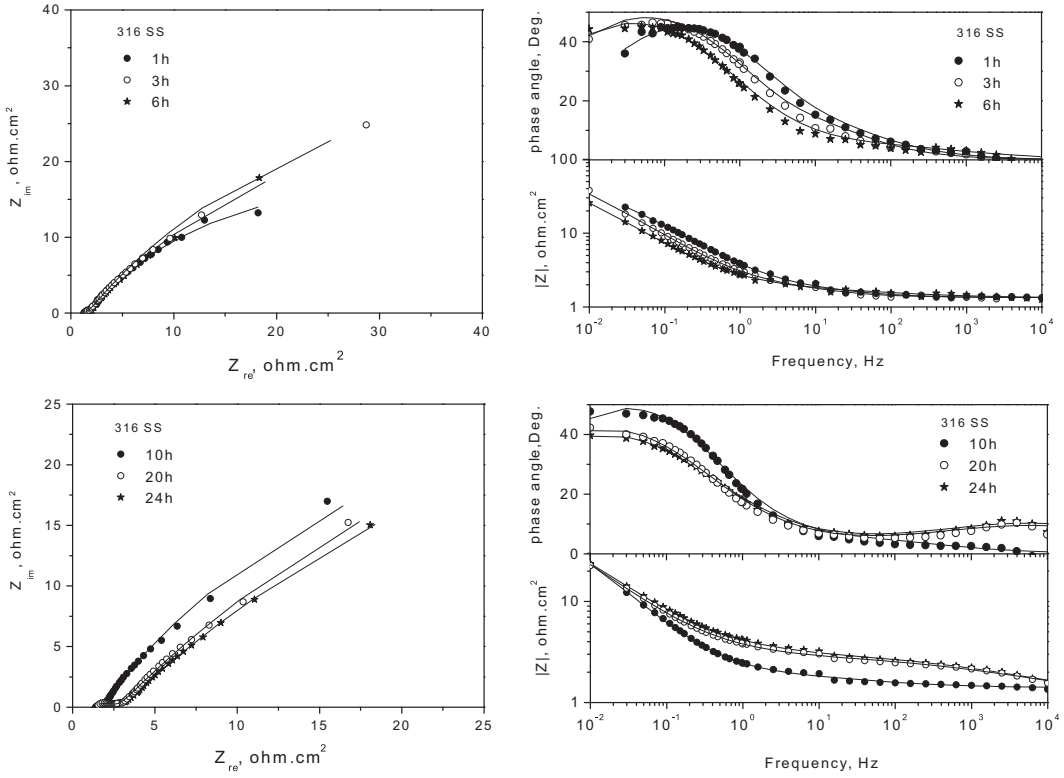

Fig. 4. Nyquist and Bode plots for the corrosion of 316SS in molten $(0.62Li, 0.38K)_2CO_3$ at 650 °C after exposure for various lengths of time. Symbol: experimental data; line: simulation data.

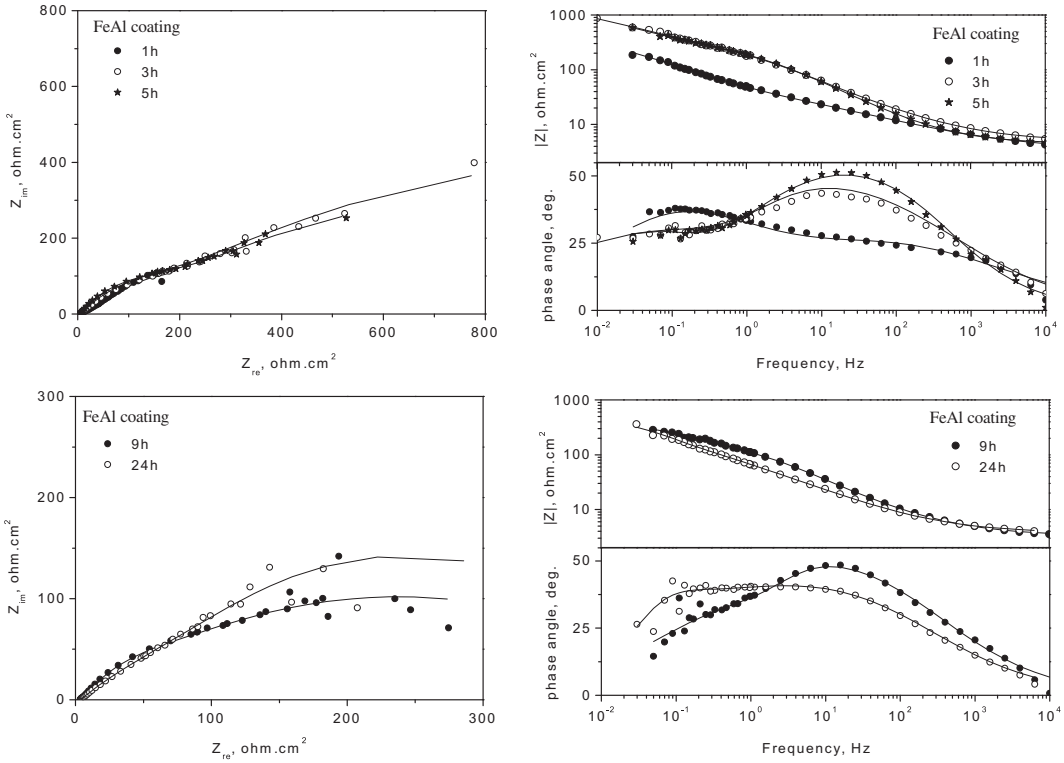

Fig. 5. Nyquist and Bode plots for the corrosion of the FeAl-coated 316SS in molten $(0.62Li, 0.38K)_2CO_3$ at 650 °C after exposure for various lengths of time. Symbol: experimental data; line: simulation data.

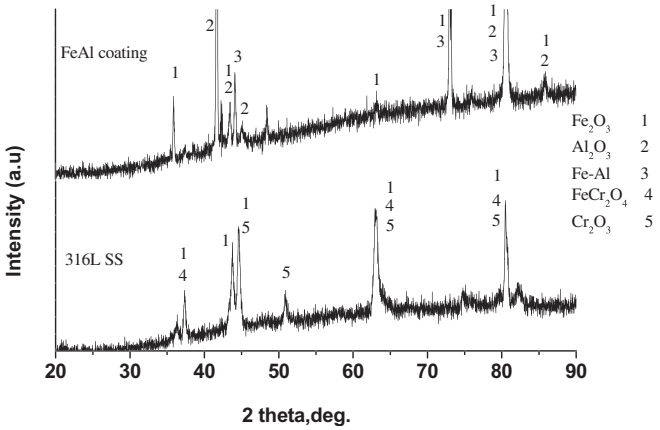

Fig. 6. X-ray diffraction patterns for the corrosion products formed on the bare and FeAl-coated 316SS after corrosion in molten $(0.62Li, 0.38K)_2CO_3$ at 650 °C for 24 h.

molten-salt resistance, C_{dl} the double-layer capacitance at the metal/melt interface, R_t the electrochemical transfer resistance, R_{ox} and C_{ox} the resistance and the capacitance of oxide scale formed on the steel, respectively. In the fitting procedure, both C_{ox} and C_{dl} were replaced with constant phase element (CPE) Q_{ox} and Q_{dl}, respectively. The impedance of CPE is expressed as

$$Z_{CPE} = \frac{1}{Y_0(j\omega)^n} \tag{1}$$

Thus, the electrochemical impedance of Fig. 8 is given by

$$Z = R_s + \frac{1}{Y_{dl}(j\omega)^{n_{dl}} + \frac{1}{R_t}} + \frac{1}{Y_{ox}(j\omega)^{n_{ox}} + \frac{1}{R_{ox}}} \tag{2}$$

where ω is the frequency, Y_0 the admittance magnitude of CPE, n the exponential term, and $0 < n < 1$. Y_{dl} and n_{dl}, Y_{ox} and n_{ox} are constants representing the elements Q_{dl} and Q_{ox} respectively.

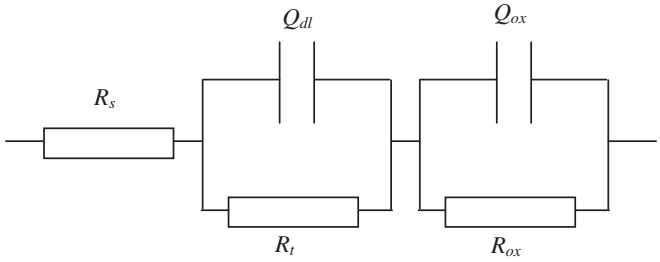

Fig. 8. Equivalent circuit for the interpretation of electrochemical impedance spectra for the corrosion of 316SS with and without FeAl coating in molten $(0.62Li, 0.38K)_2CO_3$ at 650 °C.

The electrochemical parameters in Eq. (2) can be obtained based on the equivalent circuit of Fig. 8, and the fitted results of the impedance spectra for the corrosion of the bare and FeAl-coated 316SS are listed in Tables 1 and 2, respectively. Figs. 4 and 5 show clearly that the fitting results are rather good. From Tables 1 and 2, it can be seen that the values of both R_t and R_{ox} for the coated steel are significantly larger than those for the bare steel, suggesting that the FeAl coating can increase significantly the corrosion resistance of 316SS due to the formation of a compact Al_2O_3 scale. Meanwhile, it is noted that the values of Y_{dl} and Y_{ox} for the FeAl coating are 1 ~ 2 orders of magnitude lower than those for the bare steel, which may be due to the great difference in the surface porosity and relative dielectric constant of the oxide scales formed on the bare and coated steel, respectively. The parameter Y could be approximately expressed by Eq. (3)

$$Y \approx C = \frac{\varepsilon_0 \cdot K \cdot \gamma \cdot A}{d} \tag{3}$$

where ε_0 is the dielectric constant of air, K the relative dielectric constant of the medium, γ the surface porosity, A the effective area of electrode, and d the half-thickness of capacitance. γ is an important factor that affects the value of Y. The scale porosity and electrode roughness for the bare 316SS are probably larger than

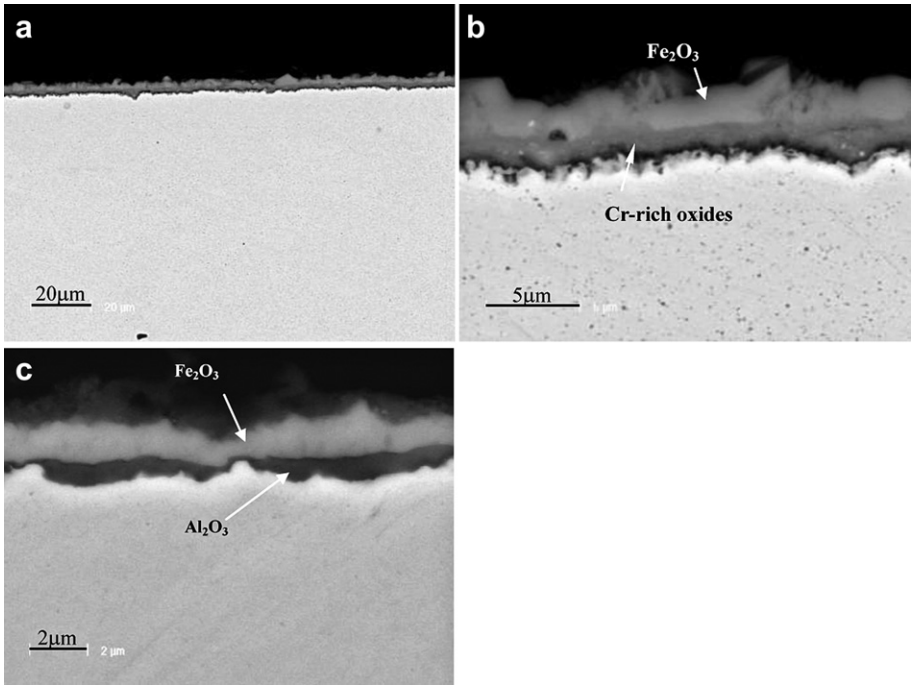

Fig. 7. Cross-sectional morphologies of 316SS (a,b) and FeAl coating (c) corroded in molten $(0.62Li, 0.38K)_2CO_3$ at 650 °C for 24 h.

Table 1
Fitting results of impedance spectra for the corrosion of 316SS in molten (0.62Li, 0.38K)$_2$CO$_3$ mixture at 650 °C after exposure for various lengths of time.

316 SS	R_s, Ω cm^2	Y_{dl}, Ω^{-1} cm^{-2} S^{-n}	n_{dl}	R_t, Ω cm^2	Y_{ox}, Ω^{-1} cm^{-2} S^{-n}	n_{ox}	R_{ox}, Ω cm^2
1 h	2.35	1.04×10^{-1}	0.71	0.24	0.10	0.67	95.48
3 h	2.35	9.14×10^{-2}	0.80	0.27	0.15	0.66	93.20
6 h	2.33	8.62×10^{-2}	0.52	0.38	0.21	0.65	88.81
10 h	2.40	9.55×10^{-2}	0.56	0.39	0.26	0.69	80.94
20 h	2.03	1.67×10^{-2}	0.37	1.80	0.25	0.62	112.75
24 h	2.02	2.89×10^{-2}	0.40	2.50	0.23	0.58	119.57

Table 2
Fitting results of impedance spectra for the corrosion of the FeAl-coated 316SS in molten (0.62Li, 0.38K)$_2$CO$_3$ mixture at 650 °C after exposure for various lengths of time.

FeAl coating on 316SS	R_s, Ω cm^2	Y_{dl}, Ω^{-1} cm^{-2} S^{-n}	n_{dl}	R_t, Ω cm^2	Y_{ox}, Ω^{-1} cm^{-2} S^{-n}	n_{ox}	R_{ox}, Ω cm^2
1 h	3.46	5.87×10^{-3}	0.45	26.11	1.08×10^{-2}	0.62	429.52
3 h	4.75	1.69×10^{-3}	0.79	84.60	3.14×10^{-3}	0.50	1025.13
5 h	4.43	1.13×10^{-3}	0.74	158.32	4.33×10^{-3}	0.57	1195.01
9 h	4.42	1.39×10^{-3}	0.64	101.21	3.57×10^{-3}	0.81	914.12
18 h	5.06	8.99×10^{-3}	0.55	92.90	8.96×10^{-3}	0.62	854.81
24 h	4.02	1.26×10^{-3}	0.62	90.54	7.59×10^{-3}	0.58	833.20

those for the FeAl-coated steel, giving rise to larger values of both Y_{dl} and Y_{ox} observed for 316SS. Though the corrosion for the bare and coated steel is all controlled by the ionic diffusion through the scale, an Al_2O_3 scale with respect to a Cr-rich scale is more effective in protecting the substrate alloy from corrosion.

As described above, several methods have been developed to prepare Al coatings for wet- seal materials. Recently, a low-cost Al-cladding method has also been developed to produce a high-quality aluminide coating, which is formed *in situ* during start-up of MCFC stacks in the temperature range between 500 and 650 °C [21]. These aluminizing processes are generally accompanied by a heat treatment. During the heat treatment, Al diffuses into the steel substrate to form intermetallic compounds. These aluminizing treatments can make the steel have sufficient aluminium for forming a protective Al_2O_3($LiAlO_2$) layer. Jun et al. [22] reported that the aluminium contents of Fe–Al alloys needed to form a stable and protective $LiAlO_2$ in the eutectic Li/K carbonate melt at 650 °C should be higher than 25 at.%. One of the present authors observed that the corrosion products formed on an Fe-24.4Al–0.12B(mass%) alloy consisted of external $LiFeO_2$ and inner Al_2O_3 in the eutectic (Li,K)$_2$CO$_3$ melt at 650 °C [20]. By comparing the results of the reference 20 and the present study, it was found that a protective Al_2O_3 scale was formed more preferentially on the FeAl coating prepared by HEMAA than on the cast FeAl. This is ascribed to the microcrystalline structure of the as-prepared FeAl coatings. HEMAA is a micro-welding process, with a high cooling rate of around 10^5–10^6 KS^{-1}. During deposition, microstructure coarsening and solute segregation could be suppressed to obtain a homogeneous microcrystalline coating with a grain size significantly smaller than that of the deposition electrode. The reduction in the grain size helps to enhance the diffusion of Al along the grain boundaries to contribute the growth of a continuous Al_2O_3 scale and to improve the adhesion of the formed scale. As compared with other aluminizing methods, HEMAA is a simple and effective process for preparing diffusion coatings with a microcrystalline structure.

4. Conclusions

HEMAA has been employed successfully to prepare FeAl coatings on 316SS using cast FeAl intermetallic compound as the deposition electrode, with a metallurgical bonding between the coating and the substrate. Due to the high cooling rate during deposition process, a microcrystalline coating with a grain size clearly smaller than that of the cast FeAl was obtained. The Nyqusit plots for the corrosion of the bare and coated 316SS in molten (0.62Li, 0.38K)$_2$CO$_3$ at 650 °C were all composed of a small semi-circle at high frequencies and a large semi-circle at low-frequency port. However, the impedance values of the coated steel are significantly larger than that of the bare steel, suggesting that FeAl coating can increase greatly the corrosion resistance of 316SS due to the formation of a continuous Al_2O_3 scale more protective than the Cr-rich scale forming on 316SS. The corrosion of the bare and coated 316SS is controlled by the diffusion of species through the scale. HEMAA is a simple and effective approach for the preparation of FeAl coatings on the wet-seal materials of MCFC.

Acknowledgements

The project supported by National Natural Science Foundation of China, Grant No 50771101.

References

[1] C.L. Zeng, T. Zhang, P.Y. Guo, W.T. Wu, Corros. Sci. 46 (2004) 2183–2189.
[2] B.H. Zhu, G. Lindbergh, D. Simonsson, Corros. Sci. 41 (1999) 1497–1513.
[3] Z.P. Liu, P.Y. Guo, C.L. Zeng, J. Power Sources 166 (2007) 348–353.
[4] A.A. Attia, S.A. Salih, A.M. Baraka, Electrochim. Acta 48 (2002) 113–118.
[5] S. Randström, C. Lagergren, P. Capobianco, J. Power Sources 160 (2006) 782–788.
[6] S. Frangini, S. Loreti, Corros. Sci. 49 (2007) 3969–3987.
[7] R.A. Donado, L.G. marianowski, H.C. Maru, J.R. Selman, J. Electrochem. Soc. 131 (1984) 2535–2540.
[8] G. Lindbergh, B. Zhu, Electrochim. Acta 46 (2001) 1131–1140.
[9] T. Tzvetkoff, J. Kolchakov, Mater. Chem. Phys. 87 (2004) 201–211.
[10] A. Agüero, F.J. García de Blas, M.C. García, R. Muelas, A. Román, Surf. Coat. Technol. 146 (2001) 578–585.
[11] F.J. Perez, D. Duday, M.P. Hierro, C. Gomez, A. Aguero, M.C. Garcia, R. Muela, A. Sanchez Pascual, L. Martinez, Surf. Coat. Technol. 161 (2002) 293–301.
[12] C. Yuh, R. Johnsen, M. Farooque, H. Maru, J. Power Sources 56 (1995) 1–10.
[13] Y. Moon, D. Lee, J. Power Sources 115 (2003) 1–11.
[14] S. Frangini, A. Masci, Surf. Coat. Technol. 184 (2004) 31–39.
[15] Z.J. Feng, C.L. Zeng, J. Power Sources 195 (2010) 7370–7374.
[16] P.Y. Guo, Y. Shao, C.L. Zeng, M.F. Wu, W.L. Li, Mater. Lett. 65 (2011) 3180–3183.
[17] Y.J. Ren, C.L. Zeng, J. Power Sources 171 (2007) 778–782.
[18] A.J. Appleby, S.B. Nicholson, J. Electrochem. Soc. 112 (1980) 71–76.
[19] S.H. Lu, J.R. Selman, J. Electrochem. Soc. 137 (1990) 1125–1130.
[20] C.L. Zeng, W. Wang, W.T. Wu, Oxidat. Metals 53 (2000) 289–302.
[21] US patent, No.US2002/6,372,374 (April 16, 2002).
[22] J. Jun, J. Jun, K. Kim, J. Power Sources 112 (2002) 153–161.